ADVANCED FUNCTIONAL MATERIALS
www.afm-journal.de

Bioprocessing Device Composed of Protein/DNA/Inorganic Material Hybrid

*Taek Lee, Ajay Kumar Yagati, Junhong Min, and Jeong-Woo Choi**

Major challenges in molecular electronics include miniaturization, and the realization of a simple function to alter silicon-based electronics. It has been hard to develop a single molecular-based computing system, since such systems need complex functionality to be developed at the single-molecular level. To develop a molecular-based biocomputing system, a bioprocessing device is demonstrated that consists of recombinant azurin/DNA/inorganic material hybrid to perform the various functions in a device. A metalloprotein which exhibits redox behavior is used as a biomemory source. The redox property could be controlled with command materials (conducting nanoparticles, heavy metal ions, and semiconducting nanoparticles) to perform 'information reinforcement,' 'information regulation,' and 'information amplification' functions, respectively. This bioprocessing device could be a foundation to develop single-biomolecular-based computing systems.

1. Introduction

The semiconductor industry has been growing at a rapid rate, but the miniaturization of electronic devices has reached technological and physical limits regarding component integration, heat, shorting of devices, and efficiency.[1,2] To overcome these current limitations, molecular electronics has enabled approaches to molecular-level size control, fabrication, and the replication of silicon-based device functions. Current molecular electronics can be suitable to alternative to current silicon-based electronic devices.[3] In recent years, molecular logic gates and computational devices have received much attention, particularly in biomolecular information processing systems, which mimic the inherent properties of enzymes for the realization of bioprocessing systems.[4–6] Difficulties in developing circuits and the complexity of scaling-up can be solved easily and naturally by the application of biomolecular systems.[7–9] The processing operations are performed by biochemical reactions that proceed in solutions or at functionalized interfaces.[10] last decade, Choi's group has focused on information storage devices based on biomolecules. Previous works demonstrate basic memory functions such as storage, reading, and the resetting of information performed using metalloprotein-based biomemory devices.[11,12] Furthermore, two different metalloproteins were coupled to demonstrate multi-level storage functions of protein-based electrochemical biomemory.[13] Also, biomemory devices with various functions have been developed to overcome the limitations of silicon-based memory devices.[14] However, these reports only demonstrated basic information storage functions, also hard to perform the molecular-based computing owing to simple functionality.

To overcome this limitation of molecular electronics, herein, we have designed a new bioprocessing device that can perform various functions with a single hybrid molecule, derived from a biomemory device with a simple metalloprotein.[11] The proposed bioprocessing device has versatile functionality unavailable in current silicon-based electronic devices. Usually, organic molecular-based electronic devices operate with simple functions such as switching, which require the integration of various components.[15] However, the proposed bioprocessing device mimics the modulating function with biochemical inputs that are coupled with enzyme systems for biocatalyzing reactions, which resembles human brain organics and "action-reaction" systems. Biochemical reactions were observed as changes in the bulk material properties or structural re-organizations at the single-molecule level, which can be demonstrated in machine language, thus allowing for the expression of chemical processes in terms of computing operations instead of traditional chemical material transformations. This concept could be extended to biohybrid molecular-based biocomputing systems.[16,17]

Therefore, in this study, we developed a bioprocessing device based on a single hybrid molecule that performs 'information reinforcement,' 'information regulation,' and 'information amplification' functions. These independent functions originate

Dr. T. Lee
Research Institute for Basic Science
Sogang University
35 Baekbeom-ro (Sinsu-dong)
Mapo-gu, Seoul, 121-742, Republic of Korea
Dr. A. K. Yagati, Prof. J.-W. Choi
Interdisciplinary Program of Integrated Biotechnology
Sogang University
35 Baekbeom-ro (Sinsu-dong)
Mapo-gu, Seoul 121-742, Republic of Korea
E-mail: jwchoi@sogang.ac.kr
Dr. A. K. Yagati, Prof. J.-W. Choi
Department of Chemical and Biomolecular Engineering
Sogang University
35 Baekbeom-ro (Sinsu-dong)
Mapo-gu, Seoul, 121-742, Republic of Korea
Prof. J. Min
School of Integrative Engineering
Chung-Ang University
Heukseok-dong, Dongjak-gu, Seoul, 156-756, Korea

DOI: 10.1002/adfm.201302397

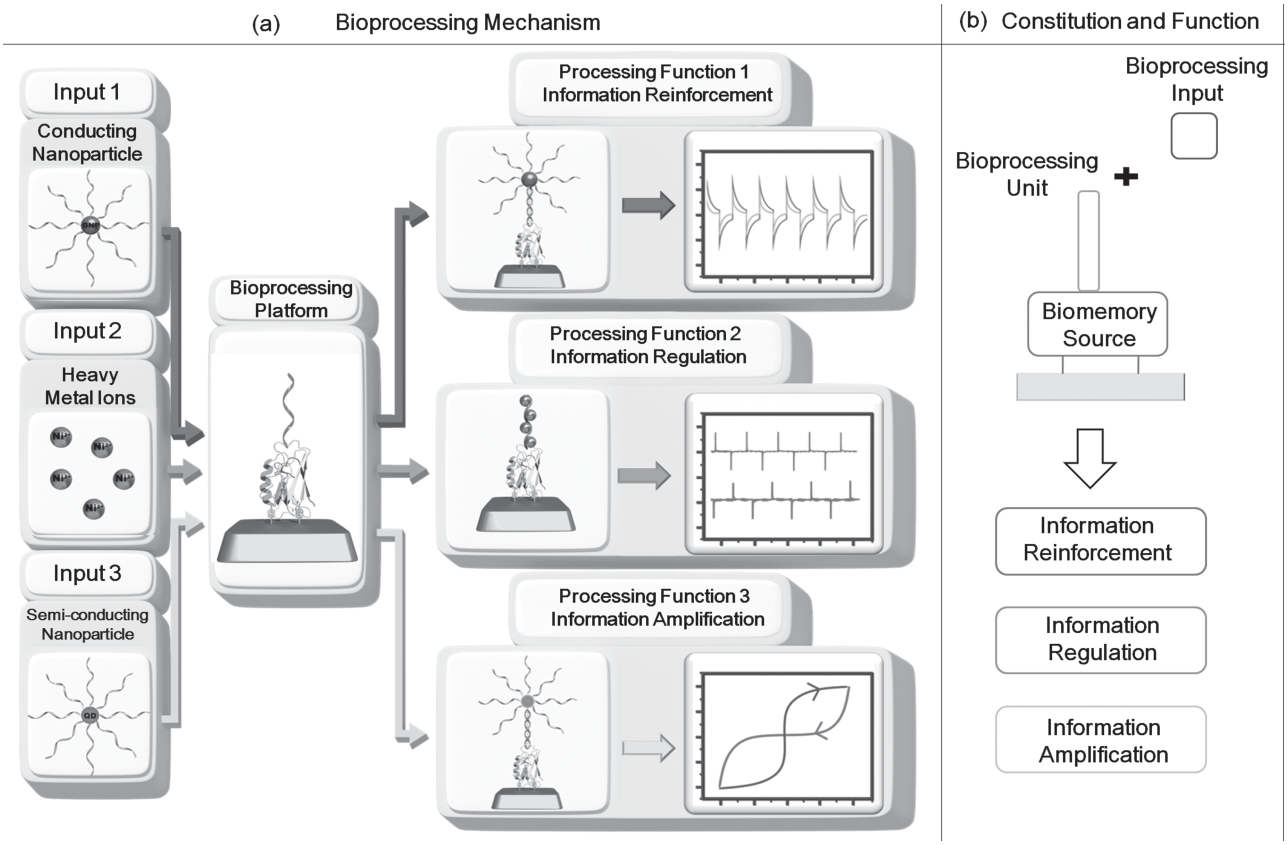

Figure 1. Schematic diagram of bioprocessing device. (a) Bioprocessing mechanism; (b) constitution and function.

from the interaction between redox properties of metalloprotein and commanding input materials. To perform these three functions on a single biohybrid material in the bioelectronic device, we designed a recombinant azurin/DNA (Azu/DNA) hybrid molecule using a chemical ligation method (CLM). **Figure 1**a shows the basic concept of the memory modulating mechanism. This mechanism shows the interaction between the redox property of metalloprotein and the input materials. Figure 1b shows the recombinant azurin utilized as a memory platform, where the DNA acts as a modulation operator. The modulation inputs can be heavy metal ions or cDNA-conducting nanoparticles coupled to the hybrid molecule. This response to modulation input was measured by cyclic voltammetry (CV), and its application was investigated by chronoamperometry (CA). Finally, the information amplification function using DNA-semiconducting nanoparticles as a modulation input was investigated using scanning tunneling spectroscopy (STS).

2. Results and Discussion

2.1. Fabrication of the Bioprocessing Device

The proposed bioprocessing device can easily assess and control various functions corresponding to the input materials in a confined region. To this end, the prepared Azu/DNA hybrid was adsorbed on an Au surface by self-assembly method. The Azu/DNA hybrid was conjugated by CLM. The conjugation method and film fabrication process are discussed in the Supporting Information (Figure S1). In sodium dodecyl sulfate-polyacrylamide gel electrophoresis (SDS-PAGE) analysis, a recombinant azurin-SMCC-DNA conjugation band (Azu/DNA hybrid) corresponding to the predicted size of the recombinant azurin-SMCC-DNA conjugate was clearly visible on the gel (**Figure 2**a, left). In the case of recombinant azurin, the molecular weight (MW) is around 14.6 kDa, and that for ssDNA (52mer) is about 16.1 kDa. The MW of the recombinant azurin-SMCC-DNA conjugate is about 30.7 kDa, confirming the formation of a high-purity recombinant Azu/DNA conjugate. Also, the recombinant azurin-SMCC-DNA conjugate concentration was determined by UV–vis measurement at 260 nm (the absorbance coefficient of the conjugate was 260 000 $M^{-1}cm^{-1}$). UV–vis spectroscopy measurements were performed to analyze the recombinant azurin-SMCC-DNA conjugate. The *pseudomonas aeruginosa* azurin, which is a blue copper metalloprotein, was selected in this study. This blue copper protein coordinates five residues (Gly45, His46, Cys112, His117, Met121), and forms a unique geometry that gives rise to a unique absorption at 627 nm Figure 2a (right: blue line).[12] In contrast, thiol-modified ssDNA does not have an intense absorption at 627 nm Figure 2a (right: green line). However, in the recombinant azurin-SMCC-DNA conjugate, the recombinant azurin retains its geometry, and the absorption at 627 nm is observed. Figure 2a (right: purple line) shows the UV spectra of the recombinant azurin. Thus, the UV–vis spectra can be

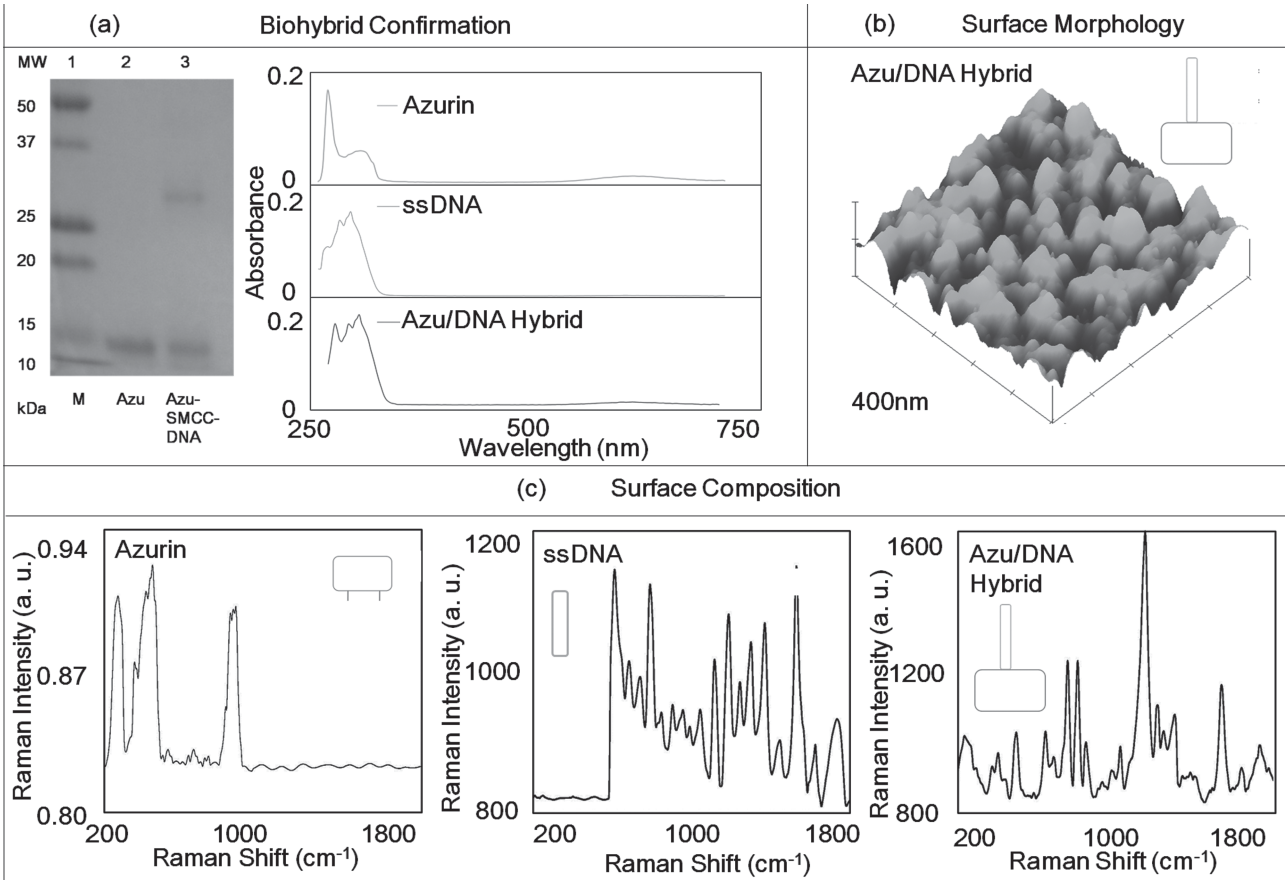

Figure 2. (a) Biohybrid confirmation: *left* SDS-PAGE, *right* UV-Vis spectroscopy. (b) Surface morphology investigation of Azu/DNA hybrid by AFM. (c) Surface composition analysis of recombinant azurin, thiol-modified ssDNA, Azu/DNA hybrid by Raman spectroscopy.

used to assess successful bioconjugation. Based on this analysis, the recombinant azurin-SMCC-DNA hybrid was shown to be produced, and it retained its unique structure. The fabrication method is described in the Supporting Information (Fabrication session). Figure 2b shows an AFM image of the Azu/DNA hybrid, and Figure 2c shows the Raman analysis of the Azu/DNA hybrid self-assembled layer. A detailed description of the AFM and Raman analysis is presented in the Supporting Information (AFM: Figure S2, Raman Spectroscopy section: Table S1).

2.2. Information Reinforcement

The concept of information reinforcement originates from electrochemical-based 2-state biomemory.[12] The 2-state biomemory was operated with two input parameters, the oxidation potential and reduction potential, which were obtained from cyclic voltamograms.CV measurements were conducted to figure out these values. **Figure 3**a depicts the CV results of the Azu/DNA hybrid and the Azu/DNA-cDNA/GNP hybrids. The reduction and oxidation potentials of the Azu/DNA hybrid are 67 ± 31 mV and 84 ± 14 mV (blue line), respectively. The results clearly show a signal enhancement in the redox property when cDNA-GNP was added to the Azu/DNA molecule. The values of oxidation and reduction potentials were found to be 232 ± 39 mV and 83 ± 68 mV (red line), respectively.

The redox properties of 3 different biomolecules were investigated as a control group (recombinant azurin, thiol-modified ssDNA, Azu/DNA hybrid). The results are described in the Supporting Information and are shown in Figure S3 and Table S2. Chronoamperometry (CA) was used to validate the information storage function. CA enabled the application of the measured oxidation potential (OP) and reduction potential (RP) to a prepared working electrode, which results in faradaic current transitions for both oxidation and reduction potentials, indicating that the device can be switched ON and OFF for charge storage functions. Using this approach, the OP and RP can be applied to working electrodes obtained in previous CV experiments. The application of OP results in electron transfer from the Azu/DNA hybrid and Azu/DNA-cDNA/GNP hybrids to the electrode, which leads to the storage of a positive charge. This state can be regarded as a 'Write' state. The application of RP enables the production of an electron transfer outflow to the Azu/DNA hybrid and Azu/DNA-cDNA/GNP hybrids, and this state can be regarded as an 'Erase' state. Applying OP and RP and measuring the current response depends on the resistance-capacitance (RC) time constant of the electrochemical system. As shown in Figure 3b, an OP step of 232 mV quantitatively oxidizes the Azu/DNA-cDNA/GNP hybrids layer (write state),

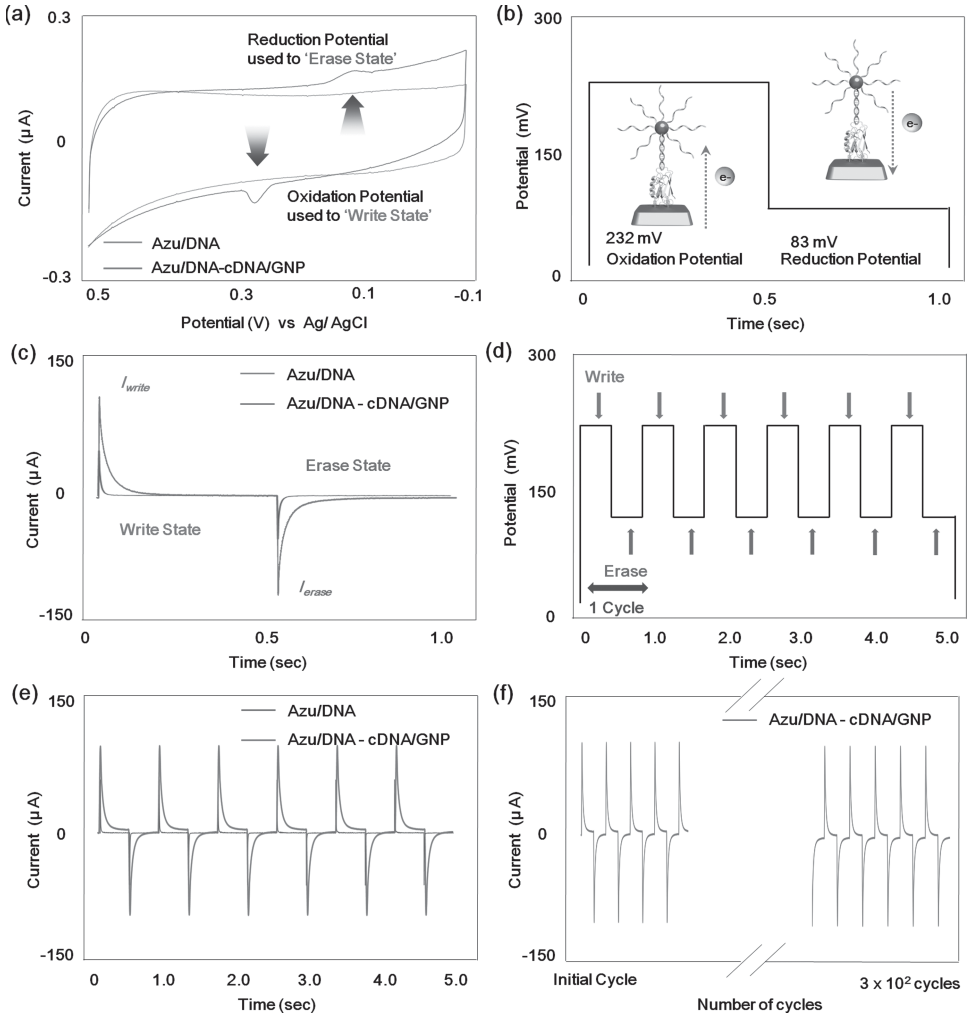

Figure 3. Information reinforcement functon when cDNA-GNP was added. (a) Cyclic voltammogram of the Azu/DNA hybrid (Blue line) and Azu/DNA-cDNA/GNP (Red line). (b) Schematic curve shows the applied sequence of potentials for ''write'' and ''erase'' functions for a total duration of 1.0 s (1 cycle), *inset*: schmatic diagram of electron inflow and outflow when cDNA/GNP was added to Azu/DNA hybrid. (c) The current response corresponding to sequence of potentials for a total duration of 1.0 s (1 cycle) (Blue line: Azu/DNA hybrid, Red line: Azu /DNA-cDNA/GNP hybrid). (d) Schematic curve shows the applied sequence of potentials for ''write'' and ''erase'' functions for a total duration of 5.0 s (6 cycles) (e) The current response corresponding to sequence of potentials for a total duration of 5.0 s (6 cycles). (f) The current response corresponding to sequence of potentials for a total duration for 3×10^2 cycles.

resulting in the storage of a positive charge in the biohybrid, and the application of an RP of 83 mV converted the layer into its original form (erase state), where the reductive current had a magnitude equal to the oxidation current. Figure 3c shows the two types of current responses, in which an OP step of 232 mV and RP of 83 mV were applied to the Azu/DNA hybrid layer, for which the conventional biomemory function was validated (Figure 3c: blue line). The function of information reinforcement was similar to the conventional biomemory function. However, when the cDNA-GNP was added to the Azu/DNA hybrid, the performance regarding the charge storage capability was drastically enhanced compared to a conventional biomemory device in the defined area (Figure 3c: red line). These characteristics can are defined as the 'information reinforcement' in a single biohybrid molecule.

With these current values, the stored charge value with the Azu/DNA hybrid could easily be estimated with Equation (1):

$$Q = \int i dt \tag{1}$$

The amount of charge stored in the Azu/DNA hybrid and Azu/DNA-cDNA/GNP hybrids by writing or erasing were calculated from the current in CA, which was found to be ~5.328 $\times 10^{-7}$ C. Similarly, the charge stored in the Azu/DNA-cDNA/GNP was calculated to be ~4.636 $\times 10^{-6}$ C. These results indicate that the charging capacity of the Azu/DNA-cDNA/GNP was increased by approximately 870% compared to the Azu/DNA hybrid. Presumably, this result was observed when the biomolecules were coupled with nanoparticles to form a bionhybrid,

and the energy levels were mixed, which favors the possibility of higher energy transfer.[18] Several groups have already reported energy level mixing and electron transfer effects when biomolecules were conjugated to nanoparticles.[19,20] This phenomenon resulted from the donor-bridge-acceptor system with electron transfer across the biomolecule-conducting nanoparticle interface.[21] This mechanism is described in the supplementary materials. With this mechanism, the information storage function can established, which was examined continuously for 6 cycles (12 steps). Figure 3d,e show a schematic diagram of the OP and RP application and the current response. This context can be regarded as Azu/DNA-cDNA/GNP having more charged current from the application of OP, RP compared to Azu/DNA hybrid. Figure 3f shows the memory performance, which was maintained for 300 cycles. The results demonstrate the stability and repeatability of the proposed information storage function. The results presented here indicate that we can easily control the information reinforcement of the Azu/DNA-cDNA/GNP hybrid. Thus, the first bioprocessing function was well established.

2.3. Information Regulation

To validate the information regulation mechanism, various input materials were added to react with the Azu/DNA hybrid to obtain the output information. With the obtained values, we can regulate the information corresponding to metal ions. To perform information regulation, the ssDNA component was used as a regulating operator. Because the binding of the ssDNA arm of the Azu/DNA to its complementary ssDNA (cDNA) molecule is highly selective, the cDNA can be a powerful tool for various applications. The ssDNA arm has a charged backbone that can bind to various heavy metal ions, such as Cu, Zn, Ni, Co, Fe, and Mn (**Figure 4**a). Thus, the ssDNA arm can be used as a regulating receptor, where input materials such as heavy metal ions can be regarded as modulating operators. DNA molecules have been shown to contain four potential sites for binding with metal ions: 1) the negatively charged phosphate oxygen atoms, 2) the ribose hydroxyls, 3) the base ring, and 4) exocyclic base keto groups. The interaction between DNA and the heavy metal ions during electron transfer play an essential role in modulating and processing the electrochemical signals. The effect of Cu(II) and Ni(II) compounds on dsDNA was previously investigated to better understand their interactions with base donor systems.[18] The electrochemical behavior of biomolecules was observed to vary in accordance with the presence of coordinated metal ions, such as Ni(II), Co(II), and Mn(II), which are located at the center of the azurin molecule.[14] In this context, we assumed that the different input materials such as heavy metal ions would strongly affect the electrochemical properties of the Azu/DNA hybrid.

The proposed bioprocessing device was operated using electrochemical methods. The basic principle of signal regulation was elucidated by electron transfer at the biomolecule-input molecule interface and the energy level perturbation of the donor-bridge-acceptor system. Perturbed energy levels will exist in the recombinant azurin-SMCC-DNA conjugate in the vicinity of the energy levels of Azurin and ssDNA. However, when input materials were added to the recombinant azurin-SMCC-DNA conjugate, a bridge was provided to facilitate the electron transfer at the DNA-Metal ions interfaces. Furthermore, the heterogeneous electron transfer is influenced by several factors, such as environmental conditions (structure/orientation, size of ions), the diffusion rate, and the injection rate. The input materials provided a bridge between the donor and acceptor system to overcome the energy levels between them. The following cell reaction describes the basic mechanism of signal regulation:

$$\text{Au/Recombinant azurin/SMCC/DNA/}^{-}\text{HEPES} - \text{H}^{+}\text{/Pt} \quad (2)$$

$$\text{Au/Recombinant azurin/SMCC/DNA/cDNA} \times\text{/Metal ions/}^{-}\text{HEPES} - \text{H}^{+}\text{/Pt} \quad (3)$$

$$\text{Au/Recombinant azurin/SMCC/DNA/cDNA} \times\text{/Nanoparticles/}^{-}\text{HEPES} - \text{H}^{+}\text{/Pt} \quad (4)$$

In contrast to reaction (2), a bridge exists in reaction (3) and reaction (4). It is likely that the various input materials such as metal ions and nanoparticles adjust the energy levels.[22–24] This phenomenon enables information regulation and reinforcement.

The reduction and oxidation potentials of the Mn ions changed from 67 ± 31 mV and 84 ± 14 mV to 413 ± 71 mV and 305 ± 47 mV; those of the Fe ions changed from 67 ± 31 mV and 84 ± 14 mV to 349 ± 52 mV and 374 ± 55 mV; those of the Co ions changed from 67 ± 31 mV and 84 ± 14 mV to 320 ± 59 mV and 350 ± 34 mV; and those of the Zn ions changed from 67 ± 31 mV and 84 ± 14 mV to 246 ± 41 mV and 334 ± 52 mV, respectively. In the case of the Ni(II) ions, the redox potential changed from 67 ± 31 mV and 84 ± 14 mV to 140 ± 22 mV and 437 ± 71 mV, and those of the Cu(II) ions, the redox potential changed from 67 ± 31 mV and 84 ± 14 mV to 106 ± 27 mV and 275 ± 34 mV. All values of redox potentials are listed in Figure 4b. The obtained OP and RP were used as memory regulating parameters. The cyclic voltammogram of each case of redox potentials specified are presented in the Supporting Information (Figure S4). Figure 4c describes the potential variation values of the Azu/DNA hybrid when various input materials were added. Figure 4c explains the reduction potential regulation when various input materials were added, as well as the oxidation potential regulation when various input materials were added compared to the oxidation potential value of the Azu/DNA hybrid.

With these regulation parameters, we can control the memory regulation by the CA method. Figure 4d depicts the regulated bioprocessing device according to the heavy metal ion inputs. When an OP of 413 mV and RP of 305 mV were applied to the Azu/DNA-Mn hybrid repeatedly, the electron was stored and erased, which was observed for a duration of 5 sec. Figure 4d (yellow line) shows the current response. The application of OP enables a charge of approximately 0.37 ± 0.12 μC to be stored at one time. When an OP of 374 mV was applied to the Azu/DNA-Fe hybrid layer, a charge of0.51 ± 0.13 μC was stored at a time. The application of an RP of 349 mV erased the information. This memory regulation step was repeated 6 times

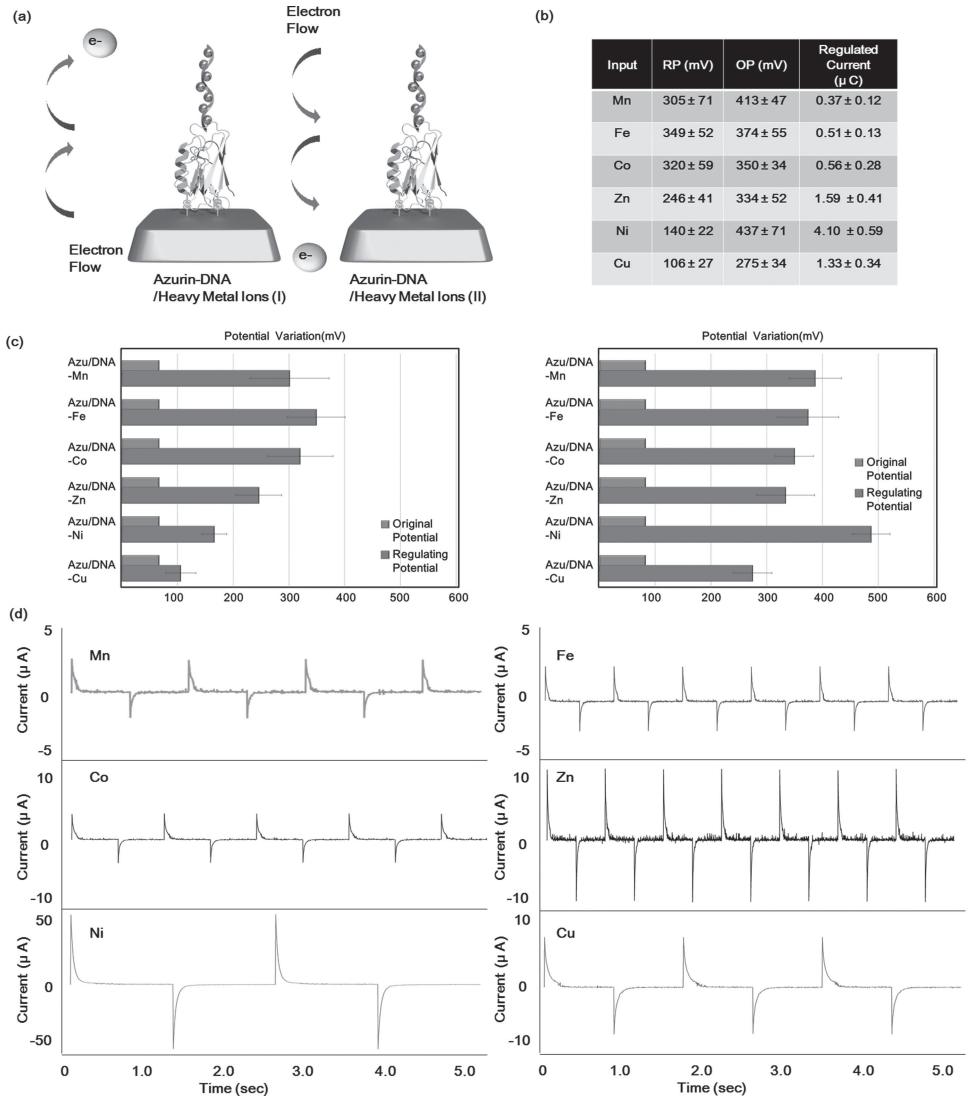

Input	RP (mV)	OP (mV)	Regulated Current (μC)
Mn	305 ± 71	413 ± 47	0.37 ± 0.12
Fe	349 ± 52	374 ± 55	0.51 ± 0.13
Co	320 ± 59	350 ± 34	0.56 ± 0.28
Zn	246 ± 41	334 ± 52	1.59 ± 0.41
Ni	140 ± 22	437 ± 71	4.10 ± 0.59
Cu	106 ± 27	275 ± 34	1.33 ± 0.34

Figure 4. Information regulation functions when various heavy metal ions were added. (a) Schematic diagram of electron flowing through the Azu/DNA-heavy metal ions. (b) Table of information modulation values when various heavy metal ions were added. (c) Left: Reduction potential regulation, Right: Oxidation potential regulation (Blue bar: original potential, Red bar: regulating potential). (d) Various information regulation result when various heavy metal ions were added. (Yellow line: Mn ions added, Purple line: Fe ions added, Navy line: Co ions added, Black line: Zn ions added, Green line: Ni ions added, Blue line: Cu ions added.)

(Figure 4d). Moreover, when an OP and RP of 350 mV and 320 mV were respectively applied to the Azu/DNA-Co hybrid, a charge 0.56 ± 0.28 μC was held and discharged for 5 sec (Figure 4d). Similarly, the Azu/DNA-Zn hybrid layer was used for memory regulation function by the application of OP (334 mV, RP 246 mV), for which a charge of 1.59 ± 0.41 μC was regulated (Figure 4d), which was repeated 7 times. In the case of the Azu/DNA-Ni hybrid (OP: 437 mV, RP: 140 mV, Figure 4d: green line), the Azu/DNA-Cu hybrid layers (OP: 275 mV, RP: 106 mV, Figure 4d) are regulated corresponding to their redox potentials. The regulated currents were 4.10 ± 0.59 μC and 1.33 ± 0.34 μC, respectively. The proposed bio-processing system composed of the protein/DNA hybrid shows the information regulation function according to various heavy metal ions with an easy method.

2.4. Information Amplification

To validate the information amplification function, we conducted scanning tunneling spectroscopy measurements on the Azu/DNA hybrid and Azu/DNA hybrid/biotin-tagged cDNA coupled with streptavidin-coated CdSe-ZnS (Azu/DNA-cDNA/QD) immobilized on an Au surface. STM is capable of high-spatial-resolution measurements. We have collected *I–V* data at several points on the Azu/DNA hybrid molecules and Azu/DNA-cDNA/QD hybrid. Our measurements show that there is a small difference in the *I–V* curves of the Azu/DNA hybrid, indicating that electron tunneling occurs via the whole molecule. **Figure 5**a shows the setup composition for scanning tunneling spectroscopy (STS), which is an effective tool for information amplification through the Azu/DNA hybrid

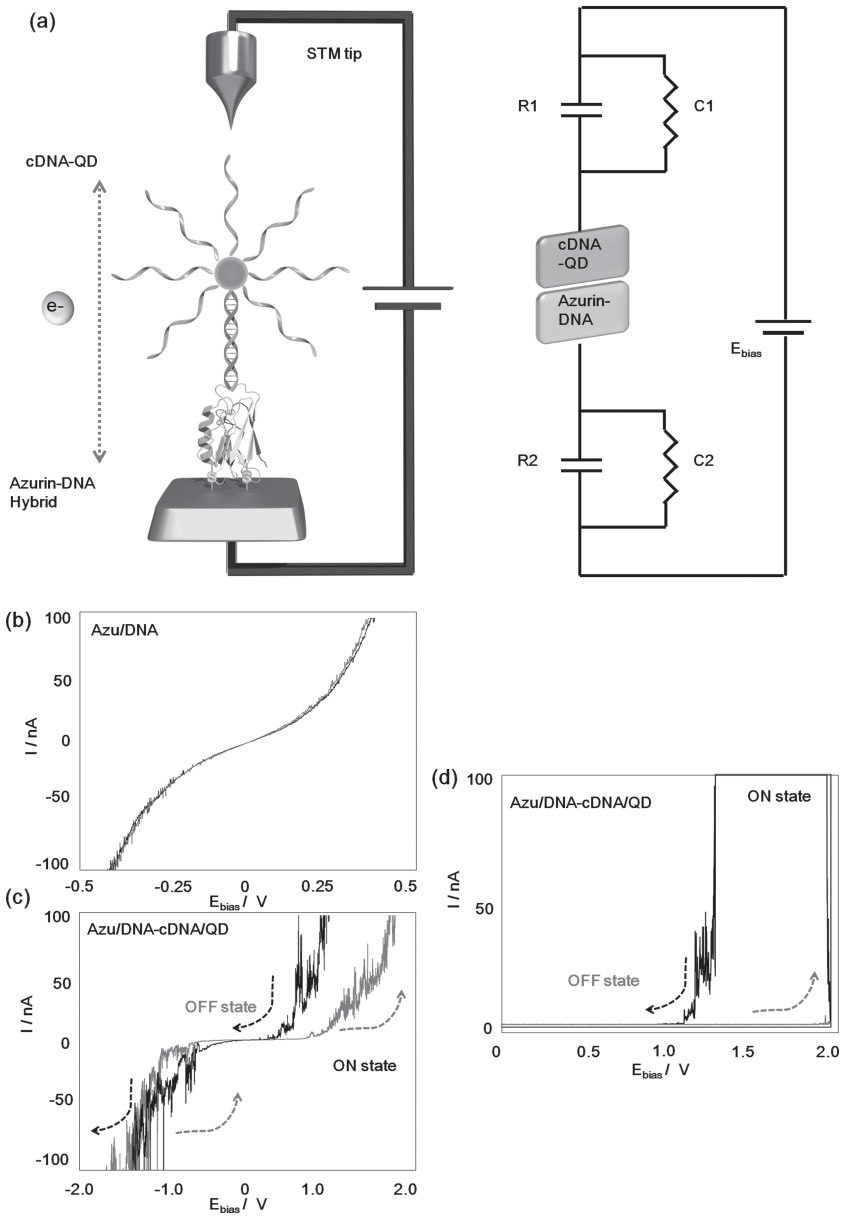

Figure 5. Information amplification function when cDNA-QD was added to Azu/DNA hybrid. (a) left one: Schematic diagram of the set-up composition of scanning tunneling spectroscopy (STS) for recombinant azurin/DNA hybrid when cDNA/semi-conducting nanoparticles. Right one: An equivalent circuit for an Azu/DNA-cDNA/QD hybrid forming a DBTJ junction between the STM and Au surface. (The schematics drawn are not adjusted to scale). (b) The I–V plot when the Azu/DNA hybrid. (c) The I–V plot when the Azu/DNA-cDNA/QD hybrid (The scan range was from –2.0 V to 2.0 V). (d) The I–V plot when the Azu/DNA-cDNA/QD hybrid (The scan range was from 0 V to 2.0 V).

in the double-barrier tunnel-junction (DBTJ) configuration. A DBTJ was realized by positioning the STM tip over the Azu/DNA hybrid, which is depicted in Figure 5a. The tunneling conductance across the junction can be measured by various potentials. Moreover, the capacitance and tunneling resistance of the tip-Azu/DNA hybrid junction (C_1 and R_1) can be easily manipulated by changing the tip hybrid distance, which is usually achieved by controlling the STM bias and current settings (V_s and I_s). The Azu/DNA hybrid junction parameters (C_2 and R_2) are practically stable. By varying C_1, one can modify the single electron charging energy, EC, which depends on the capacitance values, as well as the voltage distribution between the two junctions,[25] which is determined by the capacitance ratio, $V_1/V_2 = C_2/C_1$. Figure 5b shows an application of bias voltage from –0.5 to +0.5 V on the Azu/DNA hybrid, and depicts the semiconductor behavior. After 0.2 V of bias is applied, the Azu/DNA hybrid shows non-ohmic behavior and behaves like a diode. However, Figure 5c shows the *I-V* characteristics of Azu/DNA-cDNA/QD hybrid under the application of –2.0 to +2.0 V, which shows electrical bistability. The range of the voltage scan was kept small so as to ensure that the scanning does not induce a higher conducting state. As observed, the Azu/DNA-cDNA/QD hybrid is initially in a low conducting state (defined as the OFF state) until it reaches about 0.8 V, where an abrupt increase in the current occurs (defined as the ON state), which is equivalent to the writing process in a digital memory device. When a negative voltage of approximately –0.8 V was applied, the conjugate returned to the low conductivity state (OFF state). This change in transition from low to high conductivity is because of the charge donor azurin transferring electrons due to the Cu (I) and Cu (II) densities of states through tunneling to the lower energy core of the CdSe-ZnS core-shell nanoparticle. It is assumed that free electrons will tunnel through the conjugate by forming a double tunnel junction, which has a distribution of many energy levels sandwiched between the two metal electrodes. When the applied bias is high enough, the free electrons will tunnel through the barriers, leading to polarization with respect to the Au and Pt electrodes. As a result, the proposed bioprocessing device undergoes a dramatic change in conductance for information amplification. If the applied bias is removed, the polarized charges cannot recombine, so the device remains in the high-conductance state, where only a reverse bias can recover the device. An additional experiment considering the characteristics of I–V (Figure S5), *I-s* (Figure S6), and its derivatives (Figure S7, Table S3) are explained in the Supporting Information.

The I–V characteristics of a monolayer of the Azu/DNA-cDNA/QD hybrid core-shell nanoparticles, measured with a Pt/Ir tip of an STM under two sweep voltage directions, are shown in Figure 5d under the application of 0-2-0 V. It is clearly observed that the device switches to its high (ON) state with a sharp increase in the injection current at about

2 V, indicating the transition of the device from the low-conductivity state (OFF state) to a high-conductivity state (ON state). This transition from the OFF state to the ON state is equivalent to the writing process in a digital memory cell, which can be defined as information amplification. One of the most important features of the Azu/DNA-cDNA/QD is that the OFF state can be recovered by the simple application of a reverse voltage pulse. This is equivalent to the erasing process of a digital memory cell. Figure 5d shows the I–V characteristics of the device after the application of a revere bias. The device switched from a high conductive state to a low conductive state at 1.1 V. This bistable behavior, the OFF-ON transitions, and the creation of nonvolatile information amplification effects can be observed only in the presence of the hybrid molecules between the metal electrodes. The hybrid conjugate acts as a carrier blocking material, resulting in the blockage of electrons due to the relatively large energy barrier between the work function of the Au electrode and the HOMO level of the hybrid layer. When a positive applied voltage is applied to the electrode, after the injection of electrons from the Pt/Ir tip into the LUMO level occurs through the Fowler-Nordheim tunneling process, the electrons existing at the LUMO level are transported among the hybrid molecules along the direction of the applied bias voltage through the tunneling process. This results in the achievement of the writing process. When a negative voltage is applied to the electrode, because the electrons in the valence band of the Azu/DNA-cDNA/QD under the negative electric field are captured and then transported to the Pt/Ir electrode through the Fowler-Nordheim tunneling process, the erasing process is performed. This is equivalent to the erasing process of a digital memory cell. We have carried out the information amplification function with Azu/DNA-cDNA/QD.

3. Conclusion

In this study, we presented a novel bio-inspired bioprocessing device composed of a protein/DNA/inorganic material hybrid that could reinforce, regulate, and amplify information in single hybrid biomolecule. The proposed bioprocessing device was operated with an information reinforcing function. This function enables the storage of more charge compared to a conventional biomemory device. The information regulation can also assess the various potentials that depend on input materials. This regulation function can provide applications such as multi-bit biomemory. Additionally, information amplification can be applied to solid-state biotransistors. The proposed approach based on information control using a single hybrid biomolecule encompasses a bioprocessor concept that can perform multiple functions in a single molecule. It is usually difficult to conventional biomolecules, because of their simple characteristics and intrinsic problems, including their simple function in storing different information. However, the device presented here should be viewed as a model that provides multiple-functions in a single hybrid biomolecule. A combination of these results will pave the way to other goals such as biocomputing systems in a single hybrid biomolecule.

4. Experimental Section

Materials: The cysteine-modified azurin was expressed and purified as described previously.[12] Single-strand DNA (5′-CCCGGGAAAACCCGGGTTTTCCCGGGAAAACCCGGGTTTTCCCGAAAAAAAA-3′) was modified with a thiol-group on the 5 prime end for proper conjugation between recombinant azurin and ssDNA via sulfo-SMCC by CLM. The complementary ssDNA (5′-AACCAACCTTTTTTTT-3′) was prepared and modified with a thiol group at the 5 prime end (thiol-modified complementary-ssDNA: thiol-cDNA) for conjugation to the conducting nano particles, and biotinylated cDNA (5′-AACCAACCTTTTTTTT-3′) was prepared for streptavidin-coated CdSe-ZnS. All modified ssDNAs were supplied by Bioneer (Korea). The gold nanoparticles (GNP, 10-nm size) were purchased from BBI international (UK). Streptavidin-coated quantum dots (CdSe-ZnS, 625 nm) were purchased from Invitrogen (USA). Sulfosuccinimidyl-4-(N-maleimidomethyl) cyclohexane-1-carboxylate (Sulfo-SMCC), dithiothreitol (DTT), and Ellman's reagent were purchased from Pierce (USA). Copper(II) sulfate (Cu_2SO_4), cobalt(II) chloride ($CoCl_2$), manganese (II) sulfate monohydrate ($MnSO_4{\cdot}H_2O$), Iron (III) Oxide (Fe_2O_3), nickel chloride ($NiCl_2$), zinc sulfate ($ZnSO_4$), ethyl acetate, (4-(2-hydroxyethyl)-1-piperazineethanesulfonic acid) (HEPES), and N,N-Dimethylformamide (DMF) were purchased from Sigma Aldrich Co (USA). Distilled and deionized (DI) water was used to clean the substrates.

As a working electrode, Au substrates (Au (200 nm)/Cr (2 nm)/SiO_2 wafers) were purchased from G-mek (Korea) and used in the Raman spectroscopy, AFM, and electrochemical experiments. The Pt counter electrode and Ag/AgCl reference electrode were purchased from BAS (USA).

Information Reinforcement and Regulation: The current bioprocessing device was operated using a conventional 3-electrode system for information regulation. All electrochemical measurements were performed in a Faraday cage. The Azu/DNA hybrid immobilized Au electrode was used as a working electrode. A Pt counter electrode and Ag/AgCl reference electrode were used for the electrochemical experiments, including cyclic voltammetry and chronoamperometry. The electrochemical experiments were performed with a CHI660A electrochemical workstation (CH Instruments, USA). All results were collected under ambient conditions. During each measurement, an N_2 gas blanket was kept above the solution. Each voltammogram was scanned from the negative potential limit and increased to the positive potential limit at a scan rate of 50 mVs^{-1}.

Information Amplification: The scanning tunneling spectroscopy (STS) measurements were performed with a Digital instruments Nanoscope (R) IV (USA) at room temperature at a set point of 500 pA with 100 mV bias. The tunneling current was monitored by ramping the bias in the range of ± 2.0 V. For electrical characterization at the nanoscale, the Au substrate was used as the bottom electrode, while the 14-mm conductive STM tip was used as the top electrode for both the recombinant Azu/DNA hybrid and the recombinant Azu/DNA-cDNA/nanoparticle hybrid sandwiched in between the contacts. The STS was performed by positioning the tungsten (W) tip over an isolated recombinant Azu/DNA hybrid and recombinant Azu/DNA-cDNA/nanoparticle hybrid after disabling the feedback control.

Supporting Information

Supporting Information is available from the Wiley Online Library or from the author.

Acknowledgements

T. Lee and A. K. Yagati contributed equally to this work. We appreciate Dr. Waleed Ahmed El-Said for his efforts and advice considering Raman Analysis. This research was supported by The Nano/Bio Science &

Technology Program (M10536090001-05N3609-00110) of the Ministry of Education, Science and Technology (MEST), the National Research Foundation of Korea (NRF) grant funded by the Korea government (MEST) (2012-0000163), the Leading Foreign Research Institute Recruitment Program through the National Research Foundation of Korea(NRF) funded by the Ministry of Science, ICT & Future Planning(MSIP) (2013K1A4A3055268).

Received: July 16, 2013
Revised: October 10, 2013
Published online: December 12, 2013

[1] Y. Cui, C. M. Lieber, *Science* **2001**, *291*, 851.
[2] J. R. Heath, M. A. Ratner, *Phys. Today* **2003**, *56*, 43.
[3] C. M. Lieber, W. Lu, *Nat. Mater.* **2010**, *6*, 841.
[4] I. Willner, E. Katz, *Bioelectronics: From Theory to Applications*, Wiley-VCH, Weinheim, Germany **2005**.
[5] R. Baron, O. Lioubashevski, E. Katz, T. Niazov, I. Willner, *Angew. Chem. Int. Ed.* **2006**, *45*, 1572.
[6] E. Katz, V. Privaman, *Chem. Soc. Rev.* **2010**, *39*, **1835**.
[7] M. C. Petty, *Molecular Electronics From Principles to Practice*, Wiley, Chichester **2007**.
[8] A. Noy, *Adv. Mater.* **2011**, *23*, 807.
[9] K. Fujibayashi, R. Hariadi, S. H. Park, E. Winfree, S. Murata, *Nano Lett.* **2007**, *8*, 1791.
[10] F. C. Simmel, *ACS Nano* **2013**, *7*, 6.
[11] G. Strack, M. Pita, M. Ornatska, E. Katz, *ChemBioChem* **2008**, *9*, 1260.
[12] J.-W. Choi, B.-K. Oh, J. Min, Y. J. Kim, *Appl. Phys. Lett.* **2007**, *91*, 263902.
[13] T. Lee, S.-U. Kim, J. Min, J.-W. Choi, *Adv. Mater.* **2010**, *22*, 510.
[14] T. Lee, S.-U. Kim, J. Min, J.-W. Choi, *Biomaterials* **2011**, *32*, 3815.
[15] H. Gu, J. Chao, S.-J. Xiao, N. C. Seeman, *Nature* **2010**, *465*, 202.
[16] G. D. Ruiter, M. E. Van der Boom, *Acc. Chem. Res.* **2011**, *44*, 563.
[17] M. Amrute-Nayak, R. P. Diensthuber, W. Steffen, D. Kathmann, F. K. Hartmann, R. Fedorov, C. Urbanke, D. J. Manstein, B. Brenner, G. Tsiavaliaris, *Angew. Chem. Int. Ed.* **2010**, *49*, 312.
[18] P. N. Bartlett, *Bioelectrochemistry: Fundamentals, Experimental Techniques and Applications*, Wiley, UK **2008**.
[19] T. Pawlowski, J. Swiatek, K. Gasiorowski, H. Kozłowski, *Inorg. Chem. Acta.* **1987**, *136*, 185.
[20] P. Bhyrappa, M. Sankar, B. Varghese, *Inorg. Chem.* **2006**, *45*, 4136.
[21] I. Delfino, S. Cannistraro, *Biophys. Chem.* **2009**, *139*, 1.
[22] N. A. Anderson, T. Lian, *Annu. Rev. Phys. Chem.* **2005**, *56*, 491.
[23] J. Zhang, Q. Chi, A. G. Hansen, P. S. Jensen, P. Salvatore, J. Ulstrup, *FEBS Lett.* **2012**, *586*, 526.
[24] D. Dorokhin, N. Tomczak, D. N. Reinhoudt, A. H. Velders, G. J. Vancso, *Nanotechnology* **2010**, *21*, 285703.
[25] D. Katz, O. Millo, S. Kan, U. Banin, *Appl. Phys. Lett.* **2001**, *79*, 117.